PAPER N

WAVEFRONTS IN NON-WEAK ANISOTROPIC MEDIA

Jessé Costa

ABSTRACT

The extension of an efficient mapping algorithm based on reciprocity to anisotropic media requires the computation of wavefronts in these media. We extend the shortest path algorithm to compute wavefronts in 2-D anisotropic monoclinic media. Weak anisotropy is not assumed and the algorithm can be used with any convex slowness surfaces and arbitrary velocity contrasts.

INTRODUCTION

The general and efficient approach for obtaining XSP-CDP mapping trajectories based on reciprocity (Van Schaack, 1996) assumes only that wavefronts can be computed through the media starting at each source and receiver position. For isotropic media, a finite difference solution of the eikonal equation (Vidale, 1988) is undoubtedly the most efficient method for wavefront computation. Unfortunately this approach does not generalize easily for arbitrary anisotropy. The shortest path algorithm (Moser, 1991), although slower than finite difference approaches, can be extended easily for arbitrary anisotropy even in 3-D. The wavefront computation, based on Huygen's principle, has no limitation on high velocity contrasts. The only limitation of this approach is the requirement of convex slowness surfaces which impose restrictions on the medium in order to compute qSV wavefronts.

COMPUTATION OF WAVEFRONTS USING GRAPH THEORY

The wavefront computation using graph theory can be reduced to the determination of the shortest path between two nodes on the graph. A graph is a data structure defined by a set of nodes, a set of arcs connecting nodes, and a weight function defined on the arcs set. The shortest path problem is well known in graph theory and its solution is given by the

Dijkstra algorithm (Moser, 1991). The graph structure for the wavefront computation in this implementation is shown in Figure 1. The medium is discretized using homogeneous rectangular cells with the graph nodes regularly distributed along the cell's edges. The arcs consists of the straight rays connecting the nodes through the cell. The weight function is the traveltime along the arcs.

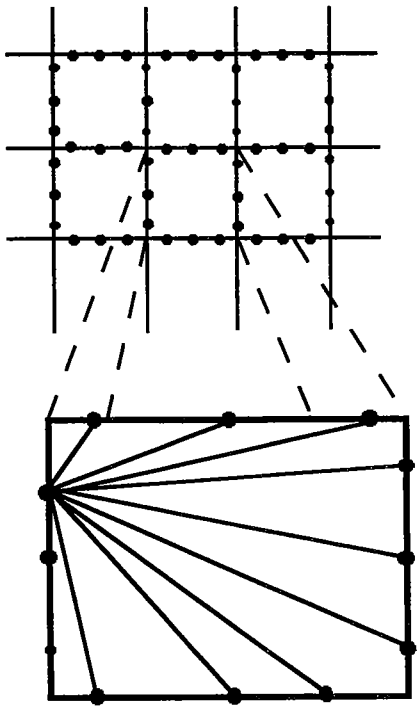

Figure 1: Graph structure for wavefront computation. The detail shows the arcs connecting the nodes in a forward start set.

Dijkstra Algorithm

A description of the Dijkstra algorithm requires some definitions (Klimec and Kvasnika, 1994). Let $\mathbf{N}$ be the set nodes and $\mathbf{A} \subset \mathbf{N} \times \mathbf{N}$ the set of arcs defining the graph. The subset of arcs $\mathbf{F}(i)=\{j \mid [i,j] \in \mathbf{A}\}$ define the forward star of the i'th node. The distance function, $\mathbf{A} \mapsto \Re$ where $\Re$ is the real numbers set, in this case the traveltime between the nodes i and j connected by the arc $[i,j] \in \mathbf{A}$. The algorithm is initialized setting the traveltime at the nodes to a large value except at the source nodes which are initialized to zero. Let $\mathbf{S}$ be the set of nodes defining the source, $\mathbf{T}$ the set of nodes with minimum traveltime already determined, $\mathbf{Q}$ the set of nodes connect to at least one node in $\mathbf{T}$, and $\mathbf{E}$ the remaining nodes in the graph. The Dijkstra algorithm for the solution of the shortest path problem is:

1 - Initialization:

$\mathbf{T}=\varnothing$, $\mathbf{Q}=\mathbf{S}$, $\mathbf{E}=\mathbf{N}-\mathbf{S}$

$\tau(\mathbf{S}) = 0$; $\tau(i)=BIG\ \forall\ i \in \mathbf{E}$.

2 - Selection:

Find i in **Q** with minimum τ,

3 - Update:

$\forall\ j \in \mathbf{F}(i) \cap \mathbf{Q}$: $\tau(j)=\min\{\tau(j), \tau(i)+d(i,j)\}$;

$\forall\ j \in \mathbf{F}(i) \cap \mathbf{E}$: $\tau(j)=\tau(i)+d(i,j)$ and add j to **Q**.

Remove i from **Q** to **T**;

If $\mathbf{Q}=\varnothing$ stop else go to step (2).

At the end of the iterations the minimum traveltime from the source to every single node is stored in the array τ (i). Following Moser (1991), the HEAPSORT algorithm (Press et al, 1990) is used in the selection step.

Traveltime between two points in anisotropic models

The complete information about the medium where the propagation occurs is contained in the arcs weights d(i,j). Therefore, the extension of the algorithm to anisotropic media is reduced to the computation of the traveltime between two nodes in a homogeneous cell. This problem is completely determined by the dispersion relation of the medium,

$$F(\mathbf{s},\eta) = 0, \tag{1}$$

where **s** is the slowness vector and η is the tensor of parameters with the density normalized elastic properties of the medium. The slowness vector associated with the straight ray connecting the nodes i and j, located at $\mathbf{x}_i = (x_i, z_i)$ and $\mathbf{x}_j = (x_j, z_j)$, is constrained by two conditions:

1) the ray direction must be normal to the slowness surface, e.g.,

$$(\mathbf{x}_j - \mathbf{x}_i) \times \nabla_s F = 0; \tag{2}$$

2) the slowness vector must obey the dispersion relation, Eqn 1.

This nonlinear system is solved using the Newton-Raphson approach (Press, 1990). In this implementation the dispersion relation for qP-qSv waves propagating at the plane of symmetry of a monoclinic medium is used:

$$F_{qP-qSv} \equiv (a_{11}s_x^2 + a_{55}s_z^2 + 2a_{15}s_x s_z - 1)(a_{55}s_x^2 + a_{33}s_z^2 + 2a_{35}s_x s_z - 1) - [a_{15}s_x^2 + a_{35}s_z^2 + (a_{13} + a_{55})s_x s_z - 1]^2 = 0 \tag{3}$$

where $a_{IJ} \equiv C_{IJ}/\rho$ is the density normalized elastic constant (Musgrave, 1970). The initial value of the slowness vector for the Newton-Raphson iterations is taken from the weak anisotropy approximations for the slowness surfaces (Costa, 1995) evaluated at the ray direction,

$$F_{qP_a} \equiv \left[C + D\cos 2\theta - \Delta \sin^2 2\theta - 2\psi \sin 2\theta + \varphi \sin 4\theta - 1/s^2\right] = 0, \tag{4}$$

$$F_{qSv_a} \equiv \left[C + \Delta \sin^2 2\theta - \varphi \sin 4\theta - 1/s^2\right] = 0, \tag{5}$$

with,

$$\begin{aligned} C &\equiv \frac{a_{11} + a_{33}}{2} \\ c &\equiv a_{55} \\ D &\equiv \frac{a_{11} - a_{33}}{2} \\ \Delta &\equiv \frac{C - (a_{13} + 2a_{55})}{2} \\ \psi &\equiv \frac{a_{15} + a_{35}}{2} \\ \varphi &\equiv \frac{a_{15} - a_{35}}{2} \end{aligned} \tag{6}$$

where θ is the angle measured with respect to the x-axis.

The process converges in 2 to 3 iterations even for strongly anisotropic media. The only requirement is the convexity of the slowness surface, which is always satisfied for qP waves. Once the slowness vector is computed the traveltime between the nodes is obtained from

$$\tau_{ij} \equiv d(i,j) = \mathbf{s} \cdot (\mathbf{x}_j - \mathbf{x}_i). \tag{7}$$

This procedure is used to compute the weight of the arcs used in the shortest path algorithm.

EXAMPLES

Wavefronts compute with the shortest path algorithm have the same accuracy as finite difference solutions of the eikonal equation (Moser, 1994). In order to evaluate the accuracy of this implementation, anisotropic wavefronts were computed in the homogeneous medium shown in Figure 2. The medium has density normalized elastic parameters close to a typical shale which are the main source of strong anisotropy in sediments. This is most likely one of the worst cases for the graph method since the straight rays cannot be represented exactly in the graph solution. The principal axis of the symmetry plane was rotated 45° for these tests. The medium was discretized in 70x140 square cells 5 ft on each side. The exact solution was obtained computing the traveltime between the source and every cell corner in the mesh using the procedure described in the previous section. The shortest path solution for the qP wavefronts and the percent error are plotted in Figure 3. The number of nodes in the cell's corners used to compute these figures were 7 and 11 respectively. The equivalent picture for the qS wavefront is shown in Figure 4. Except near the source, the percent error is smaller than 0.3% using only 7 nodes per cell's edge.

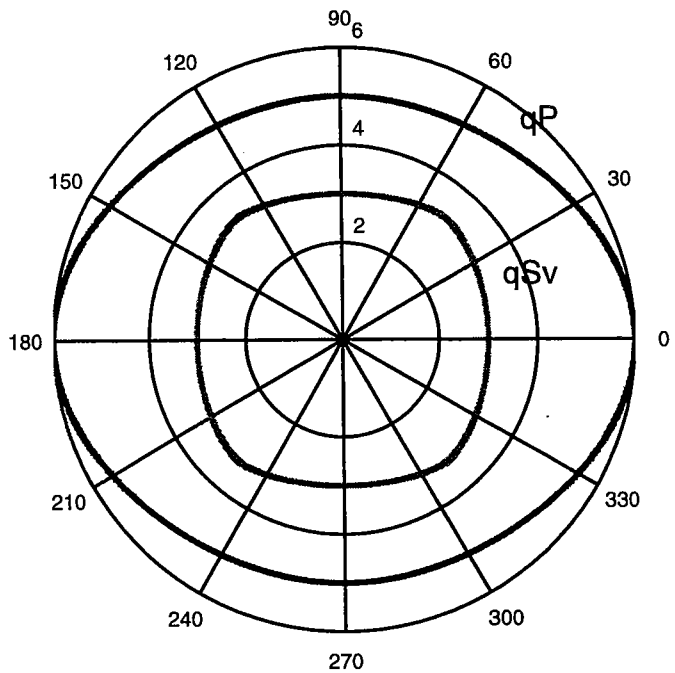

Figure 2. Group velocity surfaces for quasi-P and quasi-Sv waves. The medium has density normalized elastic parameters close to a typical shale with $a_{55}\,a_{11}$ = 36 kf/s, a_{13} = 8 kf/s, a_{33} = 25 kf/3 and a_{55} = 9 kf/s.

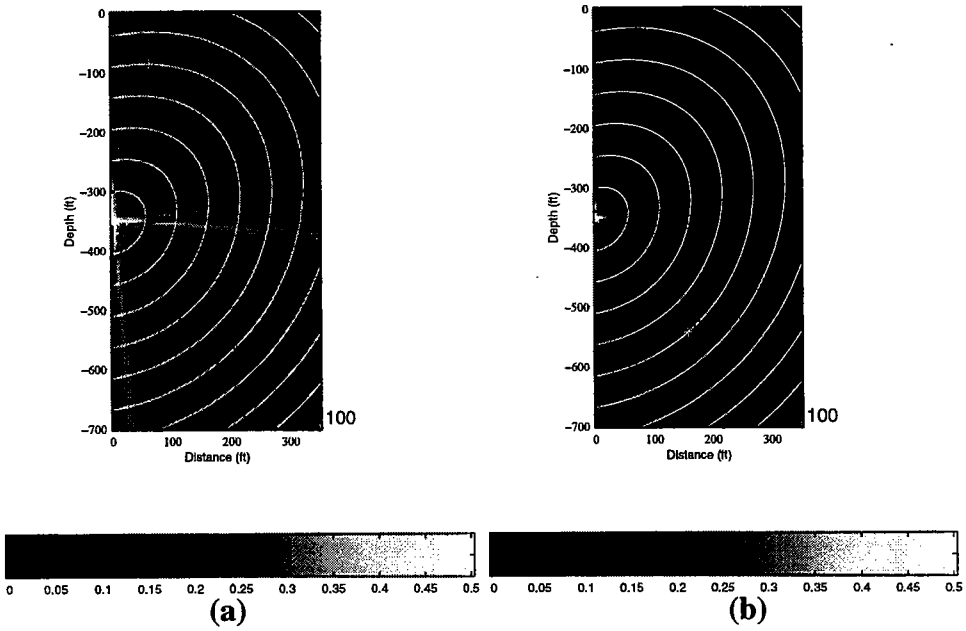

Figure 3. Shortest-path results for qP wavefronts in the medium of Fig. 1. The gray scale indicates the percent error in the solution. **(a)** shows the results using 7 nodes along each cell's edge. The example shown in **(b)** was computed using 11 nodes per edge.

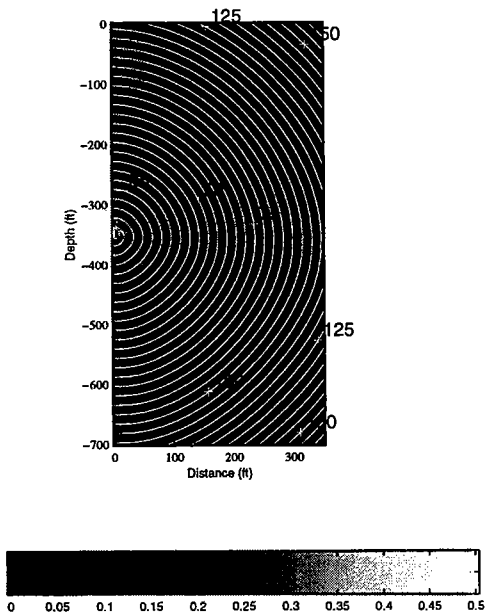

Figure 4. Wavefronts for the qSv waves computed using 11 nodes per cell's edge. The percent error is shown in grayscale.

These results suggest that the shortest path solutions have sufficient accuracy for crosswell applications. The inversion formalism for anisotropic tomography developed last year (Costa, 1995) combined with the mapping algorithm using wavefronts (Van Schaack, 1996) provides a consistent set of the tools for including anisotropy in crosswell imaging.

DISCUSSION

The shortest path method for calculating wavefront maps has the advantage of being easily extendible to include anisotropy and arbitrary mesh geometry, even for 3-D models. This is an important feature for the representation and computation of wavefronts in complex models. The only limitation for anisotropic applications is the requirement of convex slowness surfaces. Although this is always the case for qP wavefronts, qSv waves can have non-convex slowness surfaces associated with triplications on the wavefront. The accuracy of the method is the same as the finite difference solution of the eikonal equation. The main drawbacks of the approach are its large memory requirements and the slow performance compared to finite-difference wavefront computations.

REFERENCES

Klimes, L. and Kvasnicka, M., 1994, 3-D network raytracing. Geophys. J. Int., **116**, 726–738.

Costa, J. C., 1995, Traveltime tomography in anisotropic media: STP-**6**, Paper F.

Moser, T. J., 1991, Shortest path calculation of seismic rays: Geophysics, **56**, 56–67.

Moser, T. J., 1994, Migration using the shortest-path method: Geophysics, 59, 1110–1120.

Musgrave, J. P., 1970, Crystal acoustics: London. Holden-Day. 288p.

Van Schaack, M., 1996, XSP-CDP mapping in complex media without raytracing: STP-**7**, Paper O.

Vidale, J., 1988, Finite-difference calculation of traveltimes: BSSA, **78**, 2062–2076.